# Malaysian Journal of Analytical Sciences (MJAS)



Published by Malaysian Analytical Sciences Society

# SYNTHESIS AND MOLECULAR DOCKING SIMULATION OF CINNAMIC ACIDS DERIVATIVES AGAINSTS DENV2 NS2B/NS3

(Sintesis dan Simulasi Pengedokan Terbitan Asid Sinamik Terhadap DENV2 NS2B/NS3)

Nadia Mohamed Yusoff<sup>1</sup>, Siti Nor Khadijah Addis<sup>1</sup>, Nurul Huda Abdul Wahab<sup>1,2</sup>, Fauziah Abdullah<sup>3</sup> and Asnuzilawati Asari<sup>1,2,\*</sup>

<sup>1</sup>Faculty of Science and Marine Environment, Universiti Malaysia Terengganu, 21030 Kuala Nerus, Terengganu, Malaysia 
<sup>2</sup>Advanced Nano Materials (ANoMA) Research Group, Faculty of Science and Marine Environment, Universiti Malaysia 
Terengganu, 21030 Kuala Nerus, Terengganu, Malaysia

<sup>3</sup>Phytochemistry Programme, Natural Products Division, Forest Research Institute Malaysia (FRIM), 52109 Kepong, Selangor Darul Ehsan, Malaysia

\*Corresponding author: asnu@umt.edu.my

Received: 18 February 2024; Accepted: 23 April 2024; Published: 29 June 2024

#### Abstract

Dengue virus (DENV) is known as one of the serious global threats to human health since its emergence in the past few decades. However, clinically approved antiviral drugs are still not available for DENV treatment. The increased number of cases reported yearly had led to the on-going research in finding an effective drug for dengue. Cinnamic acid is a naturally occurring compound which consists of  $\alpha$ ,  $\beta$ -unsaturated carboxylic acid and is known for its wide pharmacological properties. Cinnamic acid derivatives such as caffeic acid are one of constituents in Carica papaya leaf which are used as a folk remedy for dengue. Recently, cinnamic acid was reported to show a potential against dengue virus. In this study, eight cinnamic acid derivatives were synthesized by incorporating cinnamic acid and amide moieties through the reaction of cinnamic acid with corresponding amines. All compounds were characterized by using <sup>1</sup>H and <sup>13</sup>C nuclear magnetic resonance (NMR), Fourier transform infrared (FTIR), mass spectrometry (MS) and CHN elemental analysis. Then, the synthesized compounds were simulated for molecular docking to investigate their binding affinity with the Wichapong homology protein model crystal structure, DENV-2 NS2B/NS3pro. The lower the value of FEB of a compound, the higher its binding affinity towards protein. The in-silico study revealed that compounds 6b1-6b4, with tert-butyl substituents had the highest binding affinity and good interaction with DENV-2 NS2B/NS3 serine protease. This might be due to the presence of a tert-butyl moiety in the structure, which could interact with amino acid residue of protease, thereby increasing the binding interaction between the ligand and the protein. Compound 6b2 showed the lowest FEB value despite having less H-bond interactions as compared to compound 6b3. This was probably due to the presence of more non-covalent interaction and closer bond distance which helped to enhance its binding stability. In summary, this study showed that cinnamic acid could be a promising candidate for the development of antiviral drugs to target DENV.

Keywords: cinnamic acid, synthesis, anti-dengue virus, docking

#### Abstrak

Virus denggi (DENV) telah dikenali sebagai salah satu ancaman global yang serius terhadap kesihatan manusia setelah

### Yusoff et al.: SYNTHESIS AND MOLECULAR DOCKING SIMULATION OF CINNAMIC ACIDS DERIVATIVES AGAINSTS DENV2 NS2B/NS3

kemunculannya beberapa dekad yang lalu. Walau bagaimanapun, masih belum ada ubat antiviral yang diluluskan secara klinikal bagi rawatan DENV. Peningkatan jumlah kes yang dilaporkan setiap tahun telah membawa kepada penyelidikan yang berterusan dalam pencarian ubat yang berkesan untuk rawatan denggi. Asid sinamik adalah bahan semulajadi yang mempunyai kumpulan asid karbosilik α, β-tak tepu dan dikenali dengan pelbagai sifat farmakologinya. Asid sinamik seperti asid kafeik merupakan antara komposisi yang terkandung di dalam daun Carica papaya yang digunakan secara tradisional untuk rawatan denggi. Kebelakangan ini, asid sinamik telah dilapor menunjukkan potensi terhadap DENV. Di dalam kajian ini, lapan terbitan asid sinamik telah disintesis dengan menggabungkan asid sinamik dan amida melalui tindak balas asid sinamik dengan amina yang bersesuaian. Semua sebatian dicirikan dengan menggunakan 1H and <sup>13</sup>C Resonans Magnetik Nuklear (RMN), Inframerah Transformasi Fourier (FTIR), spektrometri jisim (MS) dan analisis unsur CHN. Sebatian yang disintesis kemudiannya disimulasikan menerusi pengedokan molekul bagi mengkaji keafinan pengikatan mereka bersama struktur kristal homologi protein Wichapong, DENV-2 NS2B/NS3pro. Kajian in siliko menunjukkan bahawa sebatian 6b1-6b4, yang mengandungi kumpulan penukargantian tert-butil menunjukkan tenaga pengikatan yang tinggi dan interaksi yang baik dengan DENV-2 NS2B/NS3 serine protease. Ini mungkin disebabkan oleh kehadiran tert-butil dalam strukturnya, yang boleh berinteraksi dengan asid amino protein, dengan itu meningkatkan interaksi pengikatan antara ligan dan protein. Semakin rendah nilai FEB sebatian, semakin kuat ikatannya dengan enzim. Sebatian 6b2 menunjukkan nilai FEB terendah walaupun ia mempunyai kurang interaksi ikatan H-bond berbanding dengan sebatian 6b3, dan ini mungkin disebabkan oleh kehadiran interaksi non-kovalen yang banyak dan jarak ikatan yang berdekatan telah membantu meningkatkan kestabilan ikatannya. Secara keseluruhannya, kajian ini menunjukkan bahawa sebatian asid sinamik berpotensi untuk pembangunan ubat-ubatan antiviral bagi merawat DENV.

Kata kunci: asid sinamik, sintesis, anti-denggi, pengedokan

### Introduction

Dengue virus (DENV) is the most significant virus in the *Flaviviridae* family with the highest morbidity and mortality rates and has been a serious global threat in the past few decades [1]. The latest statistics from the World Health Organization (WHO) have shown an increasing trend of DENV infection throughout Malaysia with 127,407 reported cases in 2019 [2]. Despite this alarming issue, no current effective vaccine or antiviral treatment is available for treating dengue patients. Prevention against DENV infection by large depends on mosquito vectors control as well as the use of a natural remedy [3, 4, 5]. This underscores an urgent need to discover and develop a novel antiviral agent that is safe and effective in controlling dengue infection.

Cinnamic acid has gained a lot of interest due to its unique structure with great potential for pharmacological properties. It is a group of aromatic carboxylic acids which appear naturally in the plant kingdom. Cinnamic acids occur in all green plants as well as the reproductive organs of flowering plants [6]. Cinnamic acids with varied substitutions on the aryl ring and their esters have been identified in natural bee products, including honey and propolis [7]. It is also readily available from coffee beans, tea, cocoa, apples, tomatoes and cereals [8]. It is a safe and extensive source

of material due to its natural and low toxicity properties.

Cinnamic acid and its related molecules have a variety of biological activities, such as anticancer, antimalarial, and antimicrobial [9, 10, 11]. Additionally, cinnamic acid was also reported to be an effective antiviral drug against Zika virus (ZIKV) by inhibiting RNA-dependent RNA polymerase (RdRp) activity at the post-entry stage of ZIKV replication cycle [12]. Cinnamic acid was also reported to have excellent activity against Tobacco mosaic virus (TMV) and Hepatitis C virus (HCV) [13,14]. Despite their rich medicinal tradition and remarkable biological activities, the antiviral activity of cinnamic acid related molecules against DENV infection remained underutilised for several decades. To our knowledge, cinnamic acid derivatives were first evaluated for their anti-dengue activity and were reported by Rees and co-workers in 2008. Zosteric acid (para-sulfoxy-cinnamic acid), derived from Zostera Marina and CF238, was found to exhibit the process of virus entry. It was suggested to entrap the virus on the surface of the cell in a non-permissive binding mode and prevent the fusion process of the virus into the cell [15]. Recently, a new cinnamic acid, 3-(2-chlrophenyl) acrylic acid was synthesised based on the structural scaffold found in Carica papava, in which the extract was used as a folk remedy for dengue [16]. It was

reported that the compound showed higher inhibition activities against DENV2 NS2B-NS3 protease as compared to quercetin [17]. Arylcyanoacrylamide, aminobenzamide and  $\alpha$ -ketomide were also reported to have a significant inhibitory effect on dengue protease

NS2b/NS3 [18, 19, 20]. Due to this, this study aimed to develop a dengue inhibitor by incorporating cinnamic acid with amide, which has been reported to show potential towards DENV.

Figure 1. Structure of zosteric acid, CF238, 3-(2-chlorophenyl) acrylic acid, arylcyanoacrylamide, aminobenzamide and α-ketomide.

DENV is a single-stranded RNA genome which encodes a single open reading frame (5-C-prM-E-NS1-NS2A-NS2B-NS3-NS4A-NS4B-NS5-3) with three structural and seven non-structural proteins [21]. The N-terminal of NS3 is a trypsin-like serine protease, in which when combined with its co-factor (NS2B) it can cleave the viral polyprotein. Disruption of NS2B-NS3 protease inhibits viral replication [22]. This poses NS2B-NS3 protease of DENV-2 as a promising target for antiviral drug design [23]. The three catalytic triad amino acid residues present in NS3 serine proteases were His51, Asp75 and Ser135. The NS2B protease acted as an NS3 serine protease co-factor for an optimal catalytic activity [24]. The homology protein crystal structure generated by Wichapong et al. (2010) was used due to lack of DENV-2 NS2B/NS3 serine protease inhibitor-bound 3D

structures. Moreover, some protease database structures were found to have missing amino acid residues [25].

In the selection of an effective medicine for patient, in addition to having a high biological activity, the targeted molecule must exhibit low toxicity and adhere to druglike properties as outlined in Lipinski's Rule of Five. These properties, such as molecule size, hydrogen bonding characteristic and lipophilicity, play a crucial role in determine the permeability of molecule throughout the body [26]. Evaluation for these ADME (for absorption, distribution, metabolism, and excretion) parameter can be evaluated using SwissADME web tool [27].

In this study, eight cinnamic acid derivatives were synthesised, characterised, and subjected to molecular docking simulations to investigate their binding interactions with the protein target of DENV-2 NS2B/NS3 protease. The drug-likeness parameter of compounds was calculated by using SwissADME.

#### **Materials and Methods**

#### Chemicals and instrumentations

The chemicals and solvents used were purchased from Sigma-Aldrich Co., Acros Organics, QRec and Merck Chemical Co. (Reagent Grade) and were used without further purification. Thin-layer chromatography (TLC) was performed on a plastic-backed pre-coated with silica gel plates (Merck silica gel, 60 F254), in the solvent system of ratio Hexane:ethylacetate (7:3). Completion of the reaction was determined by the appearance of product and disappearance of reactant spots under UV-fluorescence ( $\lambda_{max}$ = 254 nm), respectively. All reactions were carried out in heat-dried glassware under dry nitrogen atmosphere by using a ballon, unless otherwise stated. All liquids transferred were conducted by using standard cannula techniques. All spectral data were obtained on the following instruments: Attenuated total reflected-infrared (ATR-IR) spectra were recorded by using Perkin Elmer 100 spectrometer model at a spectral range of 4000-400 cm<sup>-1</sup>. <sup>1</sup>H (400 MHz) and <sup>13</sup>C (100 MHz) Nuclear magnetic resonance spectra were obtained on Bruker Avance II 400 spectrometer and were reported in unit ppm on the  $\delta$  scale. NMR analyses used DMSO-d<sub>6</sub> and

TMS solvents as the internal standards. The data were analyzed by using Bruker TopSpin software package. The chemical shift was internally referenced to solvent DMSO-d<sub>6</sub> ( $^{1}$ H  $^{8}$  2.50;  $^{13}$ C  $^{8}$  39.5). The mass spectrometer experiments were performed by using LCMS Orbitrap Discovery (Thermo Scientific), electrospray (ES) negative mode and the samples were dissolved in methanol.

### Preparation of cinnamic acid derivatives

The cinnamate-amide derivatives (**6a1-6a4** and **6b1-6b4**) were synthesized according to the reported literature procedure with slight modifications [28]. A substituted cinnamic acid (2.0 mmol) was added to 15 mL tetrahydrofuran (THF) and treated with 1-(3-Dimethylaminopropyl)-3-ethylcarbodiimide

hydrochloride (EDC.HCl) (3.0 mmol, 0.575g) under a nitrogen atmosphere. The solution was stirred at 0 °C for 30 min, and 2.0 mmol of amine was slowly added within 15 min. Then, the solution was stirred overnight at room temperature under nitrogen atmosphere. The completion of the reaction was monitored using TLC (Hexane: ethyl acetate, 7:3). The solvent was removed under reduced pressure, and the residue was treated with water and extracted with ethyl acetate. The organic extract was washed with 5% HCl solution, 5% NaHCO<sub>3</sub> solution and brine. The organic layer was dried over MgSO<sub>4</sub>, filtered, and then evaporated under reduced pressure. The reactions are illustrated in Scheme 1.

Scheme 1. Preparation of cinnamic acid amide derivatives (6a1-6a4 and 6b1-6b4)

### 3-(4-hydroxyphenyl)-N-4-phenylacrylamide (6a1)

Pale brownish powder (0.272g, 56.8%), m.p.156 °C (lit. 156 °C, [29]), compound 6a1 was prepared from the reaction of 4-hydroxycinnamic acid (0.33g, 2.0 mmol) with aniline (0.19g, 2.0 mmol) in the same manner as described in Scheme 1. Data analysis: <sup>1</sup>H NMR (400 MHz, DMSO-d<sub>6</sub>):  $\delta_H$  ppm, 10.12 (1H, s, NH), 9.98 (1H, s, OH), 7.67-7.75 (2H, m, H-ar), 7.48-7.56 (3H, m, H-ar and CH), 7.29-7.38 (2H, m, H-ar), 7.06 (1H, t, J= 8.0 Hz, H-ar), 6.86 (2H, d, J= 12.0 Hz, ), 6.66 (1H, d, J= 16.0 Hz, CH);  ${}^{13}$ C NMR (100 MHz, DMSO-d<sub>6</sub>): δ<sub>C</sub> ppm, 116.3 (2×CH-ar), 119.1 (=CH), 119.6 (2×CH-ar), 123.6 (CH-ar), 126.2 (Cq), 129.2 (2×CH-ar), 130.0 (2×CHar), 140.0 (Cq), 140.8 (=CH), 159.7 (C-O), 164.5 (C=O); FTIR (ATR, cm<sup>-1</sup>): v 3317 (N-H, secondary amide), 3022 (O-H, phenol), 2922 (C-H, aromatic), 1651 (C=O), 1599 (N-H bend, secondary amide), 821 (C-H oop, aromatic); Found MS (ES, negative mode)  $[M-H]^+$  238.09  $C_{15}H_{12}NO_2$ , requires 238.27. Anal. Calculated for C<sub>15</sub>H<sub>13</sub>NO<sub>2</sub>: C, 75.30; H, 5.48; N, 5.85; Found: C, 73.55; H, 5.51; N, 5.24.

# 3-(4-hydroxyphenyl)-N-(4-methoxyphenyl) acrylamide (6a2)

Pale greenish-yellow powder (0.383g, 71.2%), m.p.167 °C, compound 6a2 was prepared from the reaction of 4hydroxycinnamic acid (0.33g, 2.0 mmol) with 4methoxyaniline (0.25g, 2 mmol) in the same manner as described in Scheme 1. Data analysis: <sup>1</sup>H NMR (400 MHz. DMSO- $d_6$ ):  $\delta_H$  ppm, 10.00 (1H, s, NH), 9.97 (1H, s, OH), 7.65 (2H, d, *J*= 8.0 Hz, H-ar), 7.53 (1H, s, H-ar), 7.46 (2H, d, J= 8.0 Hz, H-ar), 6.92 (2H, d, J= 8.0 Hz, Har), 6.85 (2H, d, J= 8.0 Hz, H-ar), 6.63 (1H, d, J= 16.0 Hz, CH), 3.74 (3H, s, OCH3); <sup>13</sup>C NMR (100 MHz. DMSO-d<sub>6</sub>):  $\delta_C$  ppm, 55.6 (OCH<sub>3</sub>), 114.4 (2×CH-ar), 116.3 (2×CH-ar), 119.2 (=CH), 121.1 (2×CH-ar), 126.3 (Cq), 129.9 (2×CH-ar), 133.1 (Cq), 140.3 (=CH), 155.6 (C-O), 159.6 (C-O), 164.1 (C=O); FTIR (ATR, cm<sup>-1</sup>): v 3328 (N-H, secondary amide), 3066 (OH, phenol), 2946 (C-H, aromatic), 1679 (C=O), 1598 (N-H bend, secondary amide), 821 (C-H oop, aromatic); Found MS (ES, negative mode) [M-H]<sup>+</sup> 268.10 C<sub>16</sub>H<sub>13</sub>NO<sub>3</sub>, requires 268.30. Anal. Calculated for C<sub>16</sub>H<sub>15</sub>NO<sub>3</sub>: C, 71.36; H, 5.61; N, 5.20; Found: C, 68.45.15; H, 5.79; N, 4.79.

### 3-(4-hydroxyphenyl)-N-(4-methylphenyl) acrylamide (6a3)

Yellowish brown powder (0.306g, 60.5%), m.p. 167 °C [29], compound 6a3 was prepared from the reaction of 4-hydroxycinnamic acid (0.33g, 2.0 mmol) with 4methylaniline (0.21g, 2 mmol) in the same manner as described in Scheme 1. Data analysis: <sup>1</sup>H NMR (400 MHz. DMSO-d6):  $\delta_{\rm H}$  ppm, 10.01 (1H, s, NH), 9.95 (1H, s, OH), 7.59 (2H, d, J= 8.0 Hz, H-ar), 7.48 (3H, t, J= 12.0 Hz, H-ar and CH), 7.13 (2H, d, J= 8.0 Hz, H-ar), 6.84 (2H, d, J= 8.0 Hz, H-ar), 6.62 (1H, d, J= 16.0 Hz, CH), 2.26 (3H, s, CH<sub>3</sub>); <sup>13</sup>C NMR (100 MHz. DMSO $d_6$ ):  $\delta_C$  ppm, 20.9 (CH<sub>3</sub>), 116.3 (2×CH-ar), 119.2 (=CH), 119.6 (2×CH-ar), 126.3 (Cq), 129.6 (2×CH-ar), 129.9 (2×CH-ar), 132.5 (Cq), 137.5 (Cq), 140.5 (=CH), 159.6 (C-O), 164.3 (C=O); FTIR (ATR, cm<sup>-1</sup>): v 3250 (N-H, secondary amide), 3012 (O-H, phenol), 2920 (C-H, aromatic), 1653 (C=O), 1594 (N-H bend, secondary amide), 816 (C-H oop, aromatic); Found MS (ES, negative mode) [M-H]+ 252.10 C<sub>16</sub>H<sub>14</sub>NO<sub>2</sub>, requires 252.30. Anal. Calculated for C<sub>16</sub>H<sub>15</sub>NO<sub>2</sub>: C, 75.87; H, 5.97; N, 5.53; Found: C, 68.45; H, 5.79; N, 4.79.

### 3-(4-hydroxyphenyl)-N-(4-chlorophenyl) acrylamide (6a4)

Yellow powder (0.352g, 64.0%), m.p. 187 °C [30], compound 6a4 was prepared from the reaction of 4hydroxycinnamic acid (0.33g, 2.0 mmol) with 4chloroaniline (0.26g, 2 mmol) in the same manner as described in Scheme 1. Data analysis: <sup>1</sup>H NMR (400 MHz. DMSO-d6):  $\delta_{\rm H}$  ppm, 10.12 (1H, s, NH), 9.98 (1H, s, OH), 7.72 (2H, d, J= 7.9 Hz, H-ar), 7.48-7.56 (2H, m, H-ar), 7.33 (2H, t, *J*= 7.7, 8.1 Hz, H-ar), 7.05 (1H, t, *J*= 7.4, 7.3 Hz, H-ar), 6.85 (2H, d, J= 8.4 Hz, H-ar), 6.66 (1H, d, J= 16.0 Hz, CH), 3.47 (1H, s, OH); <sup>13</sup>C NMR (100 MHz. DMSO-d<sub>6</sub>):  $\delta_C$  ppm, 116.3 (2×CH-ar), 118.7 (2×CH-ar), 121.1 (2×CH-ar), 127.1 (Cq), 129.1 (2×CHar), 130.1 (2×CH-ar), 138.9 (Cq), 141.2 (=CH), 159.8 (C-O), 164.6 (C=O); FTIR (ATR, cm<sup>-1</sup>): v 3367 (N-H, secondary amide), 3112 (O-H, phenol), 2925 (C-H, aromatic), 1662 (C=O), 1594 (N-H bend, secondary amide), 826 (C-H oop, aromatic); Found MS (ES, negative mode) [M-H]<sup>+</sup> 272.05 C<sub>15</sub>H<sub>11</sub>ClNO<sub>2</sub>, requires 272.72. Anal. Calculated for C<sub>15</sub>H<sub>12</sub>ClNO<sub>2</sub>: C, 65.82; H, 4.42; N, 5.12; Found: C, 65.72; H, 4.83; N, 4.75.

### 3-(4-tert-butylphenyl)-N-4-phenylacrylamide (6b1)

Pale yellow powder (0.515g, 92%), m.p.142 °C [31], compound **6b1** was prepared from the reaction of 4-tertbutylcinnamic acid (0.41g, 2.0 mmol) with aniline (0.19g, 2.0 mmol) in the same manner as described in Scheme 1. Data analysis: <sup>1</sup>H NMR (400 MHz. DMSO $d_6$ ):  $\delta_H$  ppm, 10.23 (1H, s, NH), 7.74 (2H, d, J=8.0 Hz, H-ar), 7.57 (3H, m, H-ar and CH), 7.46 (2H, d, J=12.0Hz), 7.34 (2H, t, J= 8.0 Hz, H-ar), 7.07 (1H, t, J= 8.0 Hz, H-ar), 6.84 (1H, d, J= 16.0 Hz, CH), 1.30 (9H, s,  $3 \times \text{CH}_3$ ),  $^{13}\text{C NMR}$  (100 MHz. DMSO-d<sub>6</sub>):  $\delta_{\text{C}}$  ppm, 31.4 (3×CH<sub>3</sub>), 35.0 (Cq), 119.7 (2×CH-ar), 121.9 (=CH), 123.7 (CH-ar), 126.3 (2×CH-ar), 128.0 (2×CH-ar), 129.2 (2×CH-ar), 132.5 (Cq), 139.8 (Cq), 140.5 (=CH), 153.1 (Cq), 164.2 (C=O); FTIR (ATR, cm<sup>-1</sup>): v 3314 (N-H, secondary amide), 2953 (C-H, aromatic), 1662 (C=O), 1597 (N-H bend, secondary amide), 825 (C-H oop, aromatic); Found MS (ES, negative mode) [M-H]+ 278.06 C<sub>19</sub>H<sub>20</sub>NO, requires 278.38. Anal. Calculated for C<sub>19</sub>H<sub>21</sub>NO: C, 81.68; H, 7.58; N, 5.01; Found: C, 79.87; H, 7.17; N, 5.96.

# 3-(4-*tert*-butylphenyl)-N-(4-methoxyphenyl) acrylamide (6b2)

Brown solid (0.357g, 96.2%), m.p.175 °C [31], compound **6b2** was prepared from the reaction of 4-tertbutylcinnamic acid (0.41g, 2.0 mmol) with 4methoxyaniline (0.25g, 2 mmol) in the same manner as described in Scheme 1. Data analysis: <sup>1</sup>H NMR (DMSO $d_6$ , 400 MHz):  $\delta_H$  ppm, 10.09 (1H, s, NH), 7.62-7.65 (2H, d, J= 12.00 Hz, H-ar), 7.52-7.56 (3H, t, J= 8.00, 8.00 Hz, H-ar), 7.45-7.47 (2H, d, J= 8.00 Hz, H-ar), 6.91-6.93 (2H, d, J= 8.00 Hz, H-ar), 6.76-6.80 (1H, d, J= 16.00 Hz, CH), 3.74 (3H, s, CH<sub>3</sub>), 1.28 (9H, s, $3 \times \text{CH}_3$ ). <sup>13</sup>C NMR (DMSO-d<sub>6</sub>, 100 MHz):  $\delta_C$  ppm, 31.4 (3×CH<sub>3</sub>), 35.0 (Cq), 55.6 (OCH<sub>3</sub>), 114.4 (2×CH-ar), 121.1 (2×CH-ar), 122.0 (=CH), 126.3 (2×CH-ar), 127.9 (2×CH-ar), 132.5 (Cq), 133.0 (Cq), 139.9 (=CH), 152.9 (Cq), 155.7 (C-O), 163.7 (C=O); FTIR (ATR, cm<sup>-1</sup>): v3311 (N-H, secondary amide), 2954 (C-H, aromatic), 1660 (C=O), 1597 (N-H bend, secondary amide), 825 (C-H oop, aromatic); Found MS (ES, negative mode) [M-H]+ 308.17 C<sub>20</sub>H<sub>22</sub>NO<sub>2</sub>, required 308.41. Anal. Calculated for C<sub>20</sub>H<sub>23</sub>NO<sub>2</sub>: C, 77.64; H, 7.49; N, 4.53; Found: C, 78.85; H, 7.32; N, 5.31.

### 3-(4-*tert*-butylphenyl)-N-(4-methylphenyl) acrylamide (6b3)

Yellow solid powder (0.541g, 92.3%), m.p.135 °C, compound 6b3 was prepared from the reaction of 4-tertbutylcinnamic acid (0.41g, 2.0 mmol) with 4methylaniline (0.21g, 2.0 mmol) in the same manner as described in Scheme 1. Data analysis: <sup>1</sup>H NMR (400 MHz. DMSO- $d_6$ ):  $\delta_H$  ppm, 10.15 (1H, s, NH), 7.57-7.63 (5H, m, H-ar), 7.46 (2H, d, J= 8.0 Hz, H-ar), 7.14 (2H, d, J= 8.0 Hz, H-ar), 6.82 (1H, d, J= 16.0 Hz, CH), 2.27 (3H, s, CH<sub>3</sub>), 1.28 (9H, s, 3×CH<sub>3</sub>); <sup>13</sup>C NMR (100 MHz. DMSO-d<sub>6</sub>): δ<sub>C</sub> ppm 21.0 (CH<sub>3</sub>), 31.4 (3×CH<sub>3</sub>), 35.0 (Cq), 119.7 (2×CH-ar), 122.0 (=CH), 126.3 (2×CH-ar), 128.0 (2×CH-ar), 129.6 (2×CH-ar), 132.5 (Cq), 132.7 (Cq), 153.0 (Cq), 140.2 (=CH), 163.9 (C=O); FTIR (ATR, cm<sup>-1</sup>): v 3245 (N-H, secondary amide), 2954 (C-H, aromatic), 1654 (C=O), 1605 (N-H bend, secondary amide), 816 (C-H oop, aromatic); Found MS (ES, negative mode) [M-H]+ 292.17 C<sub>20</sub>H<sub>22</sub>NO, requires 292.41. Anal. Calculated for C<sub>20</sub>H<sub>23</sub>NO: C, 81.87; H, 7.90; N, 4.77; Found: C, 83.18; H, 7.64; N, 5.47.

# 3-(4-*tert*-butylphenyl)-N-(4-chlorophenyl) acrylamide (6b4)

Pale yellow solid powder (0.439g, 69.9%), m.p.135 °C, 6b4 was prepared from the reaction of 4-tertbutylcinnamic acid (0.41g, 2.0 mmol) with 4chloroaniline (0.26g, 2.0 mmol) in the same manner as described in Scheme 1. Data analysis: <sup>1</sup>H NMR (400 MHz. DMSO- $d_6$ ):  $\delta_H$  ppm, 10.37 (1H, s, NH), 7.75 (2H, d, J= 8.9 Hz, H-ar), 7.56-7.61 (3H, m, H-ar), 7.47 (2H, d, J= 8.4 Hz, H-ar), 7.39 (2H, d, J= 8.9 Hz, H-ar), 6.79  $(1H, d, J=15.7 Hz, CH), 1.30 (9H, s, 3\times CH_3); {}^{13}C NMR$ (100 MHz. DMSO-d<sub>6</sub>):  $\delta_C$  ppm 31.4 (3×CH<sub>3</sub>), 35.0(Cq), 121.2 (2×CH-ar), 126.3 (2×CH-ar), 127.3 (=CH), 128.1 (2×CH-ar), 129.2 (2×CH-ar), 132.3 (2×Cq), 138.8 (Cq), 140.9 (=CH), 153.2 (Cq), 164.3 (C=O); FTIR (ATR, cm<sup>-</sup> 1): v 3318 (N-H, secondary amide), 2958 (C-H, aromatic), 1662 (C=O), 1594 (N-H bend, secondary amide), 824 (C-H oop, aromatic); Found MS (ES, negative mode) [M-H]<sup>+</sup> 312.12 C<sub>19</sub>H<sub>19</sub>ClNO, required 312.83. Anal. Calculated for C<sub>19</sub>H<sub>20</sub>ClNO: C, 72.72; H, 6.42; N, 4.46; Found: C, 72.02; H, 6.26; N, 5.23.

### Molecular docking

The in-silico studies (molecular docking) were conducted to investigate the binding interactions of the synthesized compounds towards DENV-2 NS2B/NS3 protease and in search for the best orientation of ligand-protease complex with the lowest free energy of binding (FEB). This step served as a good tool to predict and match the desired binding site, understand possible conformation of the compounds and further clarify the binding interactions in the binding pocket [32].

### Preparation of protein

The DENV non-structural protein homology model, NS2B/NS3pro with tetrapeptide inhibitor (Bz-Nle-Lys-Arg-Arg-H) developed by Wichapong and co-worker [33] was used as the protein target. This model was constructed based on DENV2 complex cofactorprotease and by using the crystal structure of NS2B/NS3pro West Nile Virus (WNV) as the template. Meanwhile, the coordinate was taken from DENV2 NS2b/NS3 crystal structure (PDBID: 2FOM). The NS2B/NS3pro was prepared as macromolecule prior to docking AutoDock 4.2 by using (www.autodock.scrips.edu). The protein was initially prepared by removing its inhibitor complex (Bz-Nle-Lys-Arg-Arg-H) by using Discovery Studio Client 2020 (www.accelrys.com). Both protein and ligand were prepared by using AutoDockTools 1.5.7. Kollmann charges were added to the protein structure while Gasteiger charge was added to the ligand. Both prepared protein and ligand were saved in pdbqt format file prior to docking simulation.

### Preparation of ligand

The cinnamic acid derivatives were constructed in twodimensional (2D) and three-dimensional (3D) structures and optimized by using ChemDraw Professional 16.0. The structures were saved in sdf format before being converted to pdb format.

#### **Docking analysis**

The docking simulation was performed by using AutoDock 4.2. In the positive control docking, extracted native ligand was re-docked into the binding sites of the protein. Coordinates of the redocked Bz-Nle-Lys-Arg-Arg-H were used as an active site of docking. The grid

box size of dimension  $60 \times 60 \times 60$  Å in x, y, z coordinates and grid spacing of 0.375 Å were employed to cover the protein active site. The docking of ligands was applied with Lamarckian Genetics Algorithm (GA) search program to generate 100 runs. The re-docked results with the low root mean square deviation (RMSD) value of less than 2.0 Å were applied as the fix parameter for ligands simulation.

### **ADME** properties

Lipinski's rule of five, also known as Pfizer rule is used in the prediction of a new compound to act as a drug molecule based on the membrane permeability and absorbance in the organism. The drug-likeness parameter of compounds was calculated by using a free access online server, SwissADME (http://swissadme.ch/)[27].

#### **Results and Discussion**

In this study, eight cinnamic acid amide derivatives were synthesized by the reaction of cinnamic acid with corresponding amine derivatives. EDC.HCl was used as a catalyst to produce cinnamic acid amide derivatives (6a1-6a4 and 6b1-6b4) in moderate to excellent yield (56.8-96.2%). Based on the literature, a common approach used to improve the reactivity of carboxyl group towards nucleophilic reagent is by employed a carbodiimide reaction [34, 35, 36]. The proposed plausible mechanism for the formation of cinnamic acid amide derivatives is shown in Figure 2.

The reaction starts with deprotonation of carboxylic group by EDC.HCl to form an active *O*-acylisourea intermediate. The highly electrophilic *O*-acylisourea intermediate is unstable and a good leaving group [35]. This intermediate was resonance stabilized, which then underwent a nucleophilic attack from amine to form an amide bond and removed urea by-product [36]. <sup>1</sup>H and <sup>13</sup>C NMR spectra of synthesized compounds were available in Supplementary material. The chemical shift for <sup>1</sup>H and <sup>13</sup>C NMR for **6a1-6a4** and **6b1-6b4** are tabulated in Table 1 and Table 2, respectively. The proton signal for N-H of all synthesized compounds was observed as a broad singlet at the downfield region of δ<sub>H</sub> 10.00-10.23 ppm. Compared with the literature, the proton of N-H appeared at more downfield region [29,

### Yusoff et al.: SYNTHESIS AND MOLECULAR DOCKING SIMULATION OF CINNAMIC ACIDS DERIVATIVES AGAINSTS DENV2 NS2B/NS3

30, 31]. This may be due to the temperature, concentration and solvent affecting the chemical shift of amide proton [37]. High intensity singlets of methyl and methoxy moieties in **6a1-6a4** were observed at  $\delta_{\rm H}$  2.26 and 3.74 ppm, respectively. The electronegativity of oxygen attached to CH<sub>3</sub> in the methoxy group caused it to be more deshielded and their chemical shifted downfield, as compared to methyl moieties. A similar

pattern was observed in  $^{13}$ C NMR, whereby the signal for methoxy carbonyl appeared at a more upfield region ( $\delta_{\rm C}$  20.9 ppm) than methyl carbonyl ( $\delta_{\rm C}$  55.6 ppm). The chemical shift for C=O of amide appeared at the downfield region, 163.7-164.6 ppm. The position of C-O of methoxy ( $\delta_{\rm C}$  155.6-155.7 ppm) than C-O of hydroxyl was observed at slightly upfield ( $\delta_{\rm C}$  159.6 ppm—159.8 ppm) [37].

Figure 2. Plausible mechanism for the formation of cinnamic acid amide [35]

HO R<sub>2</sub>

6a1: 
$$R_2$$
= H;
6a2:  $R_2$ = OCH<sub>3</sub>;
6a3:  $R_2$ = CH<sub>3</sub>;
6a4:  $R_2$ = CI

Figure 3. Structure of compounds 6a1-6a4

Table 1. Chemical shift <sup>1</sup>H and <sup>13</sup>C NMR for compounds 6a1-6a4

| Comp. | Chemical Shift <sup>1</sup> H NMR (δ, ppm) |           |                 |                  | Chemical Shift <sup>13</sup> C NMR (δ, ppm) |       |                    |                 |                  |
|-------|--|-----------|-----------------|------------------|---|-------|--------------------|-----------------|------------------|
|       | ОН   | N-H       | CH <sub>3</sub> | OCH <sub>3</sub> | C=O of amide                                | С-ОН  | C-OCH <sub>3</sub> | CH <sub>3</sub> | OCH <sub>3</sub> |
| 6a1   | 9.98 (s)                                   | 10.12 (s) | -               | -                | 164.5                                       | 159.7 | -                  | -               | =                |
| 6a2   | 9.97(s)                                    | 10.00(s)  | -               | 3.74 (s)         | 164.1                                       | 159.6 | 155.6              | -               | 55.6             |
| 6a3   | 9.95 (s)                                   | 10.01 (s) | 2.26 (s)        | -                | 164.3                                       | 159.6 | -                  | 20.9            | -                |
| 6a4   | 10.02 (s)                                  | 10.12 (s) | -               | -                | 159.8                                       | 159.8 | -                  | -               | -                |

The proton signal for *tert*-butyl moieties in **6b1-6b4** appeared as singlet at  $\delta_H$  1.28 to 1.30 ppm, corresponding with literature [31]. The presence of three methyl groups in the moieties caused it to be more

shielded and upfield compared to methoxy ( $\delta_H$  3.74 ppm) and single methyl moieties ( $\delta_H$  2.27 ppm) [37]. The same trend for the peak of moieties position was observed in  $^{13}$ C NMR. The presence of carbon signal

between  $\delta_C$  34.9 to 35.0 ppm observed in <sup>13</sup>C NMR for **6b1-6b4**, and it is absence for **6a1-6a4**. This peak indicated the presence of quaternary carbon (Cq) of *tert*-butyl moieties presence in **6b1-6b4**. The chemical shift of proton and carbon for all compounds is very small, except for **6a4** and **6b4**. The proton signal for NH and carbon signal for carbonyl of amide in both **6a4** and **6b4** slightly shifted more downfield compared to other

compounds. This might be due to the presence of an electronegative Cl at the para position of the aromatic ring, which caused an anisotropic effect on the ring and thus deshielded the proton of amide attached to the ring. Though the anistropic field diminishes with distance, the presence of the oxygen in the amide may also cause the NH proton to be more deshielded [37].

Figure 4. Structure of compounds 6b1-6b4

Table 2. Chemical shift <sup>1</sup>H and <sup>13</sup>C NMR for compounds **6b1-6b4** 

| Comp. | Chem                             | ical Shift <sup>1</sup> H | I NMR (δ, | ppm)             | Chemical Shift <sup>13</sup> C NMR (δ, ppm) |                                  |   |                        |      |                  |
|-------|----------------------------------|---------------------------|-----------|------------------|---|----------------------------------|---|------------------------|------|------------------|
|       | C(CH <sub>3</sub> ) <sub>3</sub> | N-H                       | СН3       | OCH <sub>3</sub> | C=O of amide                                | C(CH <sub>3</sub> ) <sub>3</sub> | Cq of<br>C(CH <sub>3</sub> ) <sub>3</sub> | C-<br>OCH <sub>3</sub> | СН3  | OCH <sub>3</sub> |
| 6b1   | 1.30 (s)                         | 10.23 (s)                 | -         | -                | 164.2                                       | 31.4                             | 35.0                                      | -                      | -    | -                |
| 6b2   | 1.28 (s)                         | 10.09 (s)                 | -         | 3.74 (s)         | 163.7                                       | 31.4                             | 35.0                                      | 155.7                  | -    | 55.6             |
| 6b3   | 1.28 (s)                         | 10.15 (s)                 | 2.27 (s)  | -                | 163.9                                       | 31.4                             | 34.9                                      | -                      | 20.9 | -                |
| 6b4   | 1.30 (s)                         | 10.37 (s)                 | -         | -                | 164.3                                       | 31.4                             | 35.0                                      | -                      | -    | -                |

The FTIR spectrum of major functional groups for 6a1-6a4 and 6b1-6b4 are portrayed in Table 3. The absorption band of N-H bending vibration stretching for secondary amide was reported to generally appear at the range of 3370 to 3170 cm<sup>-1</sup> [38]. The FTIR spectrum of synthesized compounds featured the absorption band of N-H stretching vibration at 3367 to 3245 cm<sup>-1</sup> and the absorption band of N-H bending appears around 1594 to 1605 cm<sup>-1</sup>, which implying the presence of secondary amine in the structure [37]. The high intensity of bands was due to the combination of N-H bending band with C-N stretching band. The presence of O-H in 6a1-6a4 could be observed by the presence of a broad O-H band within the range of 3022 to 3112 cm<sup>-1</sup> [29]. A strong band of carbonyl C=O of amide stretching was observed around 1654 to 1662 cm<sup>-1</sup>, corresponding with literature [29]. A prominent out-of-plane C-H bending vibrations band appeared at 808 to 869 cm<sup>-1</sup> for all compounds attributed to a para-disubstituted aromatic compound, which were in rapport with its structures [37]. The spectral of compounds obtained agreed with the

proposed structure.

Both theoretical values of synthesized compounds for MS and CHN analysis were calculated using ChemDraw Ultra 12.0. An electron spray ionization mass spectrometer (ESI) in negative mode was used to measure the mass-to-charge ratio (m/z) of the synthesized compounds in this study. The experimental m/z for all compounds agreed with the theoretical value. The elemental composition of a synthesized compound, including carbon, hydrogen, and nitrogen (CHN), provides essential information for chemical identification [39]. This study aimed to determine the molecular formula of 6a1-6a4 and 6b1-6b4 in the respect of theoretical versus the experimental results. However, the experimental results obtained show slightly different from the theoretical value. The percentage weight of carbon for 6a1, 6a2, and 6b1-6b4 varied slightly from the theoretical value by -1.75 to 2.91%. While the difference in nitrogen percentage from the theoretical value for 6a1 and 6b1-6b4 ranged

### Yusoff et al.: SYNTHESIS AND MOLECULAR DOCKING SIMULATION OF CINNAMIC ACIDS DERIVATIVES AGAINSTS DENV2 NS2B/NS3

from -0.96 to 0.61%. These discrepancies may be attributed to the presence of solvents, which contribute to the calculation of weight percentage of experimental value. The theoretical values of oxygen showed good agreement with the experimental results for all compounds. However, the slight difference observed in the experimental nitrogen value compared to the

theoretical value was maybe due to the presence of oxygen, leading to the generation of nitrogen oxide and resulting in a lower yield of nitrogen. It has also been suggested that the degree of variability in elemental result may be due to difference in the instrumental methods used for quantifying each element [40]. The data of CHN analysis are tabulated in Table 4.

Table 3. The IR absorption peaks for the synthesized compounds (6a1-6a4 and 6b1-6b4)

| Group | Wavenumber (v, cm <sup>-1</sup> ) |                |                   |      |                                  |                                       |  |
|-------|-----------------------------------|----------------|-------------------|------|----------------------------------|---------------------------------------|--|
|       | N-H<br>(secondary<br>amide)       | OH<br>(phenol) | C-H<br>(aromatic) | C=O  | N-H bend<br>(secondary<br>amide) | Out-of-<br>plane<br>C-H<br>(aromatic) |  |
| 6a1   | 3317                              | 3022           | 2922              | 1651 | 1599                             | 821                                   |  |
| 6a2   | 3328                              | 3066           | 2946              | 1654 | 1598                             | 820                                   |  |
| 6a3   | 3250                              | 3012           | 2920              | 1653 | 1598                             | 816                                   |  |
| 6a4   | 3367                              | 3112           | 2925              | 1662 | 1594                             | 826                                   |  |
| 6b1   | 3314                              | -              | 2953              | 1662 | 1594                             | 825                                   |  |
| 6b2   | 3311                              | -              | 2954              | 1660 | 1597                             | 825                                   |  |
| 6b3   | 3245                              | -              | 2954              | 1654 | 1605                             | 816                                   |  |
| 6b4   | 3318                              | -              | 2958              | 1662 | 1594                             | 824                                   |  |

Table 4. The CHN data for the synthesized compound (6a1-6a4 and 6b1-6b4)

| Element | Carbon |              | Hydrogen |              | Nitrogen |              |
|---------|--------|--------------|----------|--------------|----------|--------------|
| •       | Theory | Experimental | Theory   | Experimental | Theory   | Experimental |
|         | (%)    | (%)          | (%)      | (%)          | (%)      | (%)          |
| 6a1     | 75.30  | 73.55        | 5.48     | 5.51         | 5.85     | 5.24         |
| 6a2     | 71.36  | 68.45        | 5.61     | 5.79         | 5.20     | 4.79         |
| 6a3     | 75.87  | 76.03        | 5.97     | 5.59         | 5.53     | 5.31         |
| 6a4     | 65.82  | 65.72        | 4.42     | 4.83         | 5.12     | 4.75         |
| 6b1     | 81.68  | 79.87        | 7.58     | 7.17         | 5.01     | 5.96         |
| 6b2     | 77.64  | 78.85        | 7.49     | 7.32         | 4.53     | 5.31         |
| 6b3     | 81.87  | 83.18        | 7.90     | 7.64         | 4.77     | 5.47         |
| 6b4     | 72.72  | 72.02        | 6.42     | 6.23         | 4.46     | 5.23         |

In the positive control docking, the center of the grid box was determined by the center of Bz-Nle-Lys-Arg-Arg-H at 23.038, 3.372, -0.316 in the x, y and z coordinates, respectively. The Lamarckian genetic algorithm was employed with the covalent map parameter to constrain the molecular geometry of peptide inhibitor [41, 42]. The internal validation was done by re-docking tetrapeptide inhibitor (Bz-Nle-Lys-Arg-Arg-H) with RMSD value in the range of 1.5-2.0 Å, depending on

ligand size, which indicating that the docking was able to reproduce native conformation [43]. The redocked tetrapeptide inhibitor to DENV2 NS2B/NS3pro was observed to have a similar conformation with an initial pose of the inhibitor with RMSD value 1.98 Å, as illustrated in Figure 5. The docking parameter obtained was utilized in docking simulations of ligand-DENV2-NS2b/NS3 protease study by using the synthesized compounds as ligand.

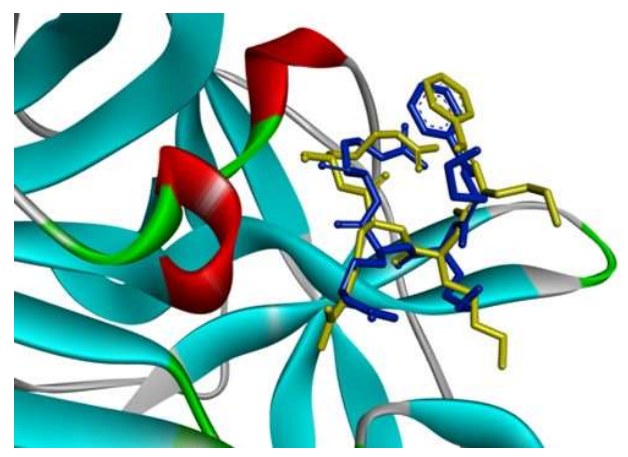


Figure 5. The overlay of the redocked Bz-Nle-Lys-Arg-Arg-H to DENV2 NS2B/NS3pro with RMSD of 1.61 Å Yellow: original; blue docked ligand conformation

The ligand-protein docking results based on free energy of binding (FEB) values and detailed type of interactions that occurred between the ligands and protease are shown in Table 5. Compounds with the lowest FEB were considered to have the strongest binding affinity towards DENV2 NS2b/NS3pro. All docked compounds displayed positive interaction with NS2b/NS3pro, with a binding energy of less than the peptide inhibitor. Generally, the difference between compounds 6a1-6a4 and 6b1-6b4 was the substitutes at the para position in the aromatic ring. The aromatic system with parasubstituent with high electron density was reported to exhibit good activity against DENV2 NS2b/NS3 [18]. The para-substituted compounds possess an advantage in molecular interaction due to their optimal conformation, favorable electrostatic interactions, lower

steric hindrance,  $\pi$ - $\pi$  stacking and hydrophobic complementary [44].

Among the eight docked compounds, ligands with *tert*-butyl substituents had the lowest free binding energies, ranging from -6.69 kcal/mol to -7.72 kcal/mol. Compounds **6b2** and **6b3** were the top two hit compounds which showed the best result with minimum FEB values of -7.72 kcal/mol and -7.26 kcal/mol, respectively. The greater negative score binding free energy indicated a stronger binding affinity between the compound and enzyme, suggesting that the compounds have a higher probability of biological activity [45, 46]. The detailed ligand-binding site interaction in 2D structural views of compounds **6b2** and **6b3** are shown in Figure 6.

Table 5. The free energy of binding (FEB) of synthesized compounds

|          |                                   | · ·         |                        |                         |
|----------|-----------------------------------|-------------|------------------------|-------------------------|
| Compound | Free Binding Energy<br>(kcal/mol) | Interaction | Type of<br>Interaction | Bond<br>Distance<br>(Å) |
| 6a1      | -6.54                             | HIS B:51    | H-Bond                 | 2.07                    |
|          |                                   | VAL B:52    | π-Alkyl                | 5.35                    |
|          |                                   | ASP B:129   | H-Bond                 | 1.92                    |
|          |                                   | PHE B:130   | H-Bond                 | 2.47                    |
|          |                                   | PRO B:132   | H-Bond                 | 4.17                    |
|          |                                   | TYR B:161   | π-π Stacked            | 1.79                    |
| 6a2      | -6.65                             | ILE B:36    | π-Alkyl                | 3.89                    |
|          |                                   | HIS B:51    | H-Bond                 | 2.03                    |
|          |                                   | VAL B:52    | π-Alkyl                | 5.36                    |
|          |                                   | ASP B:129   | H-Bond                 | 1.88                    |
|          |                                   | PHE B:130   | H-Bond                 | 2.56                    |
|          |                                   | PRO B:132   | H-Bond                 | 1.91                    |

Yusoff et al.: SYNTHESIS AND MOLECULAR DOCKING SIMULATION OF CINNAMIC ACIDS DERIVATIVES AGAINSTS DENV2 NS2B/NS3

|                        |       | TYR B:161   | π-π Stacked  | 4.13 |
|------------------------|-------|-------------|--------------|------|
| 6a3                    | -6.90 | ILE B:36    | Alkyl        | 5.37 |
|                        |       |             | π-Alkyl      | 3.98 |
|                        |       | VAL B:52    | π-Alkyl      | 5.25 |
|                        |       | ASP B:129   | H-Bond       | 2.61 |
|                        |       | PHE B:130   | H-Bond       | 2.05 |
|                        |       | PRO B:132   | H-Bond       | 1.78 |
|                        |       | TYR B:161   | π-π Stacked  | 4.69 |
| 6a4                    | -7.03 | ILE B:36    | Alkyl        | 4.42 |
|                        |       | HIS B:51    | H-Bond       | 2.09 |
|                        |       | VAL B:52    | π-Alkyl      | 5.39 |
|                        |       | ASP B:129   | H-Bond       | 1.96 |
|                        |       | PHE B:130   | H-Bond       | 2.53 |
|                        |       | PRO B:132   | H-Bond       | 1.77 |
|                        |       | TYR B:161   | π-π Stacked  | 4.09 |
| 6b1                    | -6.69 | HIS B:51    | π-Cation     | 4.41 |
|                        |       |             | π-π Stacked  | 3.73 |
|                        |       | GLY B:151   | H-Bond       | 2.06 |
| 6b2                    | -7.72 | TRP B:50    | π-Alkyl      | 5.08 |
|                        |       | VAL B:72    | Alkyl        | 4.82 |
|                        |       | ILE A:86    | Alkyl        | 4.03 |
|                        |       | GLY B:153   | H-Bond       | 2.06 |
|                        |       | VAL B:154   | π-Sigma      | 3.70 |
|                        |       | V/1L D.13 1 | Alkyl        | 4.21 |
|                        |       |             | H-Bond       | 1.89 |
|                        |       | VAL B:155   | π-Alkyl      | 5.04 |
|                        |       |             | Alkyl        | 5.13 |
| 6b3                    | 7.26  | TRP B:50    | π-Alkyl      | 5.18 |
|                        |       | HIS B:51    | π- π Stacked | 4.36 |
|                        |       | ASP B:75    | π-Anion      | 4.00 |
|                        |       | GLY B:153   | H-Bond       | 2.13 |
|                        |       | TYR B:161   | π- π Stacked | 4.03 |
|                        | 7.16  |             | π-Alkyl      | 4.00 |
| 6b4                    | -7.16 | TRP B:50    | π-Alkyl      | 5.19 |
|                        |       | HIS B:51    | π- π Stacked | 4.38 |
|                        |       | ASP B:75    | π-Anion      | 4.00 |
|                        |       | GLY B:153   | H-Bond       | 2.14 |
|                        |       | TYR B:161   | π-Alkyl      | 4.14 |
| Dogitive assets:1      |       |             | π- π Stacked | 4.07 |
| Positive control       | -5.21 | -           | -            | -    |
| (Bz-Nle-Lys-Arg-Arg-H) |       |             |              |      |
|                        |       |             |              |      |

Aside from the catalytic residue, involvement of amino acid residues, such as Val52, Val72, Pro132 and Tyr150 (in the NS3 domain) and Ile86, Gly151, Gly153 (in the NS2B cofactor domain) in ligand-protein interaction helped to contribute to the binding [47, 48]. The *tert*-butyl moiety of **6b2** and **6b3** formed an alkyl and  $\pi$ -alkyl interaction with Trp50 and Val72. Compound **6b2** and DENV2 NS2B/NS3pro complex showed H-bond interaction between O of amide with Gly153 and O of

methoxy group with Val155. The methoxy group and *tert*-butyl substituents showed non-bonding interaction of alkyl and  $\pi$ -alkyl with Val72, Ile86 and Trp50. Although no interaction occurred with the catalytic triad residues (His51, Ser135 and Asp75), the binding of 6b2 to the active site of protease was stabilized through one H-bond with Gly153 and the support of non-covalent interaction with Trp50, Val72, Ile86, Val154, and Val155. [47].

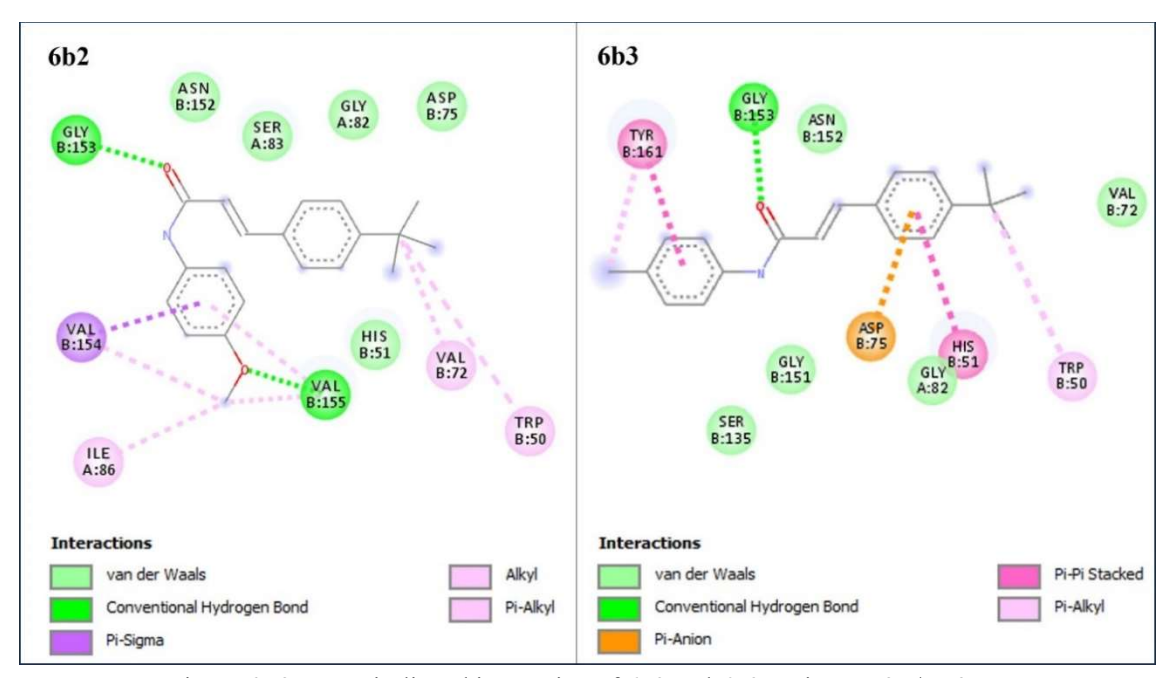


Figure 6. 2D protein-ligand interaction of 6b2 and 6b3 against NS2B/NS3pro

The docked pose showed that compound **6b3** formed one hydrogen bond interaction with Gly153 of NS3. The phenyl ring forms  $\pi$ - $\pi$  stacking and  $\pi$ -anion with catalytic triad His51 and Asp75, respectively. The ligand also formed an interaction with Tyr161 and Trp50. Even though 6b3 interacted with two catalytic triad residues, its binding free energy was slightly higher than **6b2**. This might be due to a lack of non-covalent interaction to improve binding affinity for **6b3** as compared to **6b2**. The strength of hydrogen bonding increases as it gets closer to the geometry [49]. The distance of H-bond interaction between ligand-protein for **6b2** was 2.06 Å and 1.89 Å, which is less than in

**6b3**. This made 6b2 bind more firmly to the protein, and thus its FEB value was more negative. ADME (absorption, distribution, metabolism, and excretion) describes the internal process of drug movement throughout the body. The ADME results for physiochemical properties of compounds **6b2** and **6b3** are tabulated in Table 6. The lipophilicity of drug candidate molecules was determined by the ratio of partition coefficient of n-octanol and water (log P<sub>o/w</sub>), and its value should be less than 5 for it to have good absorption [50]. The number of H-Bond donors (HBD) needed to be less than 5 and H-Bond acceptors (HBA) should be less than 10 [51, 52].

Table 6. Physiochemical properties of compounds 6b2 and 6b3

| Dyanautias —                     | The Top Two Hit Compounds |                    |  |  |  |
|----------------------------------|---------------------------|--------------------|--|--|--|
| Properties –                     | 6b2                       | 6b3                |  |  |  |
| Log S                            | -5.06                     | -5.29              |  |  |  |
| Solubility                       | Moderately soluble        | Moderately soluble |  |  |  |
| Heavy atoms                      | 23                        | 22                 |  |  |  |
| Number of rotatable bonds        | 6                         | 5                  |  |  |  |
| Number of H-bond acceptors (HBA) | 2                         | 1                  |  |  |  |
| Number of H-bond donors (HBD)    | 1                         | 1                  |  |  |  |
| Log P <sub>o/w</sub>             | 3.51                      | 3.45               |  |  |  |
| TPSA (Å <sup>2</sup> )           | 38.33                     | 29.10              |  |  |  |

According to Kenny, elimination of HBD could lead to small increases in lipophilicity and improved permeability of the molecule [53]. Topological polar surface area (TPSA) score for a drug should be less than 130 Å<sup>2</sup>, the solubility of the molecule log S, should not exceed more than 6 [54]. Both compounds were found to be within the acceptable range of drug-likeness parameter of compounds. An excessively high lipophilicity can contribute to the immobilization of the compound within a given layer [55]. Based on the ADME results, **6b2** and **6b3** were suggested to have moderate permeability against the cell barrier to be distributed to molecular targets.

### Conclusion

In conclusion, the present work has demonstrated that eight cinnamic acid derivatives were successfully synthesised through the reaction of cinnamic acid with various amines. The molecular studies revealed a significant molecular interaction between the synthesised compounds and DENV2 NS2B/NS3 protease, which indicated their potential activity as a protease inhibitor. It was observed that both compounds with a hydroxyl group and *tert*-butyl substituents displayed a high binding affinity and good interaction with DENV-2 NS2B/NS3 serine protease as compared to the tetrapeptide inhibitor (Bz-Nle-Lys-Arg-Arg-H).

Amongst the eight compounds, 6b2 and 6b3 showed the best results with the minimum value of FEB. Compound 6b2 (-7.72 kcal/mol) exhibited the lowest FEB as compared to compound 6b3 (-7.26 kcal/mol). The number of ligand-protein interactions and their distance have an important influence on the FEB value. Although hydrogen bond is deemed as important in enhancing the ligand-protein binding affinity, the bond distance, and another types of interaction, such as non-bonding interaction could also help to compensate for enhancing the binding stability and binding affinity of the ligand. The ADME results showed that compounds 6b2 and 6b3 have the potential to serve as lead molecules and be developed as inhibitors for DENV2 NS2B/NS3pro to treat dengue. However, further validation through invitro and in-vivo analysis is required.

### Acknowledgement

The authors would like to acknowledge the financial support from Ministry of Higher Education, Malaysia for Fundamental Research Grant Scheme FRGS 59580 (FRGS/1/2019/STG01/UMT/02/4). A sincere thanks to the Faculty of Science and Marine Environment, Universiti Malaysia Terengganu (UMT) for providing the research facilities.

### References

- Bhatt, S., Gething, P. W., Brady, O.J., Messina, J. P., Farlow, A. W., Moyes, C. L., Drake, J. M., Brownstein, J. S., Hoen, A. G., Sankoh, O., Myers, M. F., George, D. B., Jaenisch, T., Wint, G. R., Simmons, C. P., Scott, T. W., Farrar, J. J., and Hay, S. I. (2021). The global distribution and burden of dengue. *Nature*, 496 (7446): 504-507.
- World Health Organization (WHO). (2019).
   Dengue and severe dengue. https://www.who.int/newsroom/fact-sheets/detail/dengue-and-severe-dengue. [Access online 25 November 2020].
- Bere, A. W., Mulati, O., Kimotho, J., and Ng'ong'a, F. (2021). *Carica papaya* leaf extract silver synthesized nanoparticles inhibit dengue type 2 viral replication in vitro. *Pharmaceuticals*, 14(8): 718.
- Wong, P. F., Wong, L. P., and AbuBakar, S. (2020). Diagnosis of severe dengue: challenges, needs and opportunities. *Journal of Infection and Public He alth*, 13: 193-198.
- Khan, M., Altamish, M., Samal, M., Srivastav, V., Insaf, A., Parveen, F., Akhtar, J., Krishnan, A., and Ahmad, S. (2023). Antiviral potential of traditional unani medicine with special emphasis on dengue: A review. *Current Drug Targets*, 24(17): 1317-1334.
- Martin-Tanguy, J., Cabanne, F., Perdrizet, E., and Martin, C. (1978). The distribution of hydroxycinnamic acid amides in flowering plants. *Phytochemistry*, 17(11): 1927-1928.
- Mohammadzadeh, S., Shariatpanahi, M., Hamedi, M., Ahmadkhaniha, R., Samadi, N., and Ostad, S. N. (2007). Chemical composition, oral toxicity, and antimicrobial activity of Iranian propolis. *Food Chemistry*, 103(4): 1097-1103.
- 8. Clifford, M. N. (1999). Chlorogenic acids and other

- cinnamates nature, occurrence, and dietary burden *Journal of the Science of Food and Agriculture*, 79(3): 362-372.
- Fattah, A., Firdaus, and Soekamto, N. H. (2020). Synthesis of cinnamic acid derivative and bioactivity as an anticancer based on result quantitative structure relationship (QSAR) analysis. *Indonesia Chimica Acta*, 13(1): 23-29.
- Seck, R., Mansaly, M., Gassama, A., Cave, C. and Cojean, S. (2018). Synthesis and antimalarial activity of cinnamic acid derivatives. *Journal of Chemical and Pharmaceutical Research*, 10(11): 1-8.
- Silva, R. H., Andrade, A. C., Nóbrega, D. F., Castro, R. D. D., Pessôa, H. L., Rani, N., and de Sousa, D. P. (2019). Antimicrobial activity of 4-chlorocinnamic acid derivatives. *BioMed Research International*, 2019(1): 3941242.
- 12. Lee, S., Han, J. M., Kim, H., Kim, E., Jeong, T. S., Lee, W. S., and Cho, K. H. (2004). Synthesis of cinnamic acid derivatives and their inhibitory effects on LDL-oxidation, acyl-CoA:cholesterol acyltransferase-1 and -2 activity, and decrease of HDL-particle size. *Bioorganic and Medicinal* Chemistry Letters, 14(18): 4677-4681.
- 13. Gao, X., Tang, J., Liu, H., Liu, L., Kang, L., and Chen, W. (2018). Structure–activity relationship investigation of *tert*iary amine derivatives of cinnamic acid as acetylcholinesterase and butyrylcholinesterase inhibitors: compared with that of phenylpropionic acid, sorbic acid and hexanoic acid. *Journal of Enzyme Inhibition and Medicinal Chemistry*, 33(1): 519-524.
- Zhang, J., Yang, J., Chang, X., Zhang, C., Zhou, H., and Liu, M. (2012). Ozagrel for acute ischemic stroke: A metaanalysis of data from randomized controlled trials. *Neurological Research*, 34(4): 346-353.
- Rees, C.R., Costin, J.M., Fink, R.C., McMichael, M., Fontaine, K.A., Isern, S., and Michael, S. (2008). In vitro inhibition of dengue virus entry by p-sulfoxy-cinnamic acid and structurally related combinatorial chemistries. *Antiviral Research*, 80(2): 135-42.
- 16. Ahmad, N., Fazal, H., Ayaz, M., Abbasi, B. H., Mohammad, I., and Fazal, L. (2011). Dengue fever

- treatment with *Carica papaya* leaves extracts. *Asian Pacific Journal of Tropical Biomedicine*, 1(4): 330-333.
- Ganji, L. R., Gandhi, L., Musturi, V., and Kanyalkar, M. (2020). Design, synthesis, and evaluation of different scaffold derivatives against NS2B-NS3 protease of dengue virus. *Medicinal Chemistry Research*, 30: 285-301.
- Nitsche, C., Steuer, C., and Klein, C. D. (2011).
   Arylcyanoacrylamides as inhibitors of the dengue and West Niles virus proteases. *Bioorganic & Medicinal Chemistry*, 19(24): 7318-7337.
- Aravapalli, S., Lai, H., Teramoto, T., Alliston, K. R., Lushington, G. H., Ferguson, E. L., Padmanabha n, R., and Groutas, W. C. (2012). Inhibitors of den gue virus and West Nile virus proteases based on the aminobenzamide scaffold. *Bioorganic & Medicinal Chemistry*, 20(13): 4140-4148.
- Steuer C, GeGe C, Fischl W, Heinonen KH, Barten schlager R, Klein CD. (2011). Synthesis and biolog ical evaluation of α-ketoamides as inhibitors of the Dengue virus protease with antiviral activity in cell -culture. *Bioorganic & Medicinal Chemistry*, 19: 4 067-4074.
- 21. Leung, D., Schroder, K., White, H., Fang, N. X., Stoermer, M. J., Abbenante, G., Martin, J. L., Young, P. R., and Fairlie, D. P. (2001). Activity of recombinant dengue 2 virus NS3 protease in the presence of a truncated NS2B co-factor, small peptide substrates, and inhibitors. *Journal of Biological Chemistry*, 276(49): 45762-45771.
- 22. Chiu, M. W., Shih, H. M., Yang, T. H., and Yang, Y. L. (2007). The type 2 dengue virus envelope protein interacts with small ubiquitin-like modifier-1 (SUMO-1) conjugating enzyme 9 (Ubc9). *Journal of. Biomedical Science*, 14(3): 429-444.
- Chen, W. N., Loscha, K. V., Nitsche, C., Graham, B., and Otting, G. (2014). The dengue virus NS2B-NS3 protease retains the closed conformation in the complex with BPTI. FEBS Letters, 588(14): 2206-2211.
- 24. Tomlinson, S., Malmstrom, R., and Watowich, S. (2012). New approaches to structure-based discovery of dengue protease inhibitors. *Infectious Disorder Drug Targets*, 9(3): 327-343.
- 25. Preugschat, F., Yao, C. W., and Strauss, J. H. (1990).

- In vitro processing of dengue virus type 2 nonstructural proteins NS2A, NS2B, and NS3. *Journal of Virology*, 64(9): 4364-4374.
- Benet, L. Z., Hosey, C. M., Ursu, O., and Oprea, T. I. (2016). BDDCS, the rule of 5 and drug ability. Advanced Drug Delivery Reviews, 101: 89-98.
- 27. Daina, A., Michielin, O. and Zoete, V. (2017). SwissADME: A free web tool to evaluate pharmacokinetics, drug-likeness and medicinal chemistry friendliness of small molecules. Scientific Reports, 7: 42717.
- 28. Chai, T., Zhao, X. B., Wang, W. F., Qiang, Y., Zhang, X. Y., and Yang, J. L. (2018). Design, synthesis of N-phenethyl cinnamide derivatives and their biological activities for the treatment of Alzheimer's disease: Antioxidant, beta-amyloid disaggregating, and rescue effects on memory loss. *Molecules*, 23(10): 2663.
- Khatkar, A., Nanda, A., Kumar, P., and Narasimhan , B. (2017). Synthesis, antimicrobial evaluation and QSAR studies of p-coumaric acid derivatives. *Arab* ian Journal of Chemistry, 10: S3804-S3815.
- 30. Vishnoi, S., Agrawal, V., and Kasana, V. K. (2009). Synthesis and structure-activity relationships of su bstituted cinnamic acids and amide analogues: a ne w class of herbicides. *Journal of Agriculture and F ood Chemistry*, 57 (8): 3261-3265.
- 31. Doherty, E. M., Fotsch, C., Bo, Y., Chakrabarti, P. P., Chen, N., Gavva, N., Han, N., Kelly, M. G., Kinc aid, J., Klionsky, L., Liu, Q., Ognyanov, V. I., Tami r, R., Wang, X., Zhu, J., Norman, M. H., and Trean or, J. J. S. (2005). Discovery of potent, orally avail able vanilloid receptor-1 antagonists. Structure-acti vity relationship of n-aryl cinnamides. *Journal of M edicinal Chemistry*, 48(1): 71-90.
- 32. Grinter, S. Z., and Zou, X. (2014). Challenges, applications, and recent advances of protein-ligand docking in structure-based drug design. *Molecules*, 19(7): 10150-10176.
- Wichapong, K., Pianwanit, S., Sippl, W., and Kokpol, S. (2010). Homology modeling and molecular dynamics simulations of dengue virus NS2B/NS3 protease: Insight into molecular interaction. *Journal of Molecular Recognition*, 23(3): 283-300.
- 34. Valeur, E., and Bradley, M. (2009). Amide bond

- formation: Beyond the myth of coupling reagents, *Chemical Society Reviews*, 38: 606-631.
- 35. Kasprzak A, Zuchowska A, and Poplawska M. (2018). Functionalization of graphene: does organic chemistry matter? *Beilstein Journal of Organic Chemistry*, 14: 2018-2026.
- Liew, K. M., Tagg, T., and Khairul, W. M. (2019). S ynthesis and characterization of N-analineferrocen ylamides via carbodiimide coupling. *Malaysian Jo* urnal of Analytical Sciences, 23(2): 189-196.
- 37. Lampman, G. M., Pavia, D. L., Kriz, G. S., and Vyvyan, J. R. (2010). Spectroscopy. International Edition, Brooks/Cole Cengage Learning, Canada; pp 15-198.
- 38. Brian C. Smith. Spectroscopy Solution for Materials Analysis (2020). Multimedia Pharma Sciences, US, 35(1): pp. 10-15.
- 39. Itoh, N., Sato, A., Yamazaki, T., Numata, M., and Takatsu, A. (2013). Determination of the carbon, hydrogen and nitrogen contents of alanine and their uncertainties using the certified reference material l-alanine (NMIJ CRM 6011-a). *Analytical Sciences*, 29: 1209-1212.
- Kuveke, R. E. H., Barwise, L., van Ingen, Y., Vashisth, K., Roberts, N., Chitnis, S. S., Dutton, J. L., Martin, C. D., and Melen, R. L. (2022). An international study evaluating elemental analysis. ACS Central Science, 8(7): 855-863.
- 41. Morris, G. M., Huey, R., Lindstrom, W., Sanner, M. F., Belew, R. K., Goodsell, D. S., and Olson, A. J. (2009), AutoDock4 and AutoDockTools4: Automat ed docking with selective receptor flexibility. *Journ al of Computational Science*, 30(16): 2785-2791.
- Bianco, G., Forli, S., Goodsell, D. S., and Olson, A. J. (2016). Covalent docking using autodock: Two-point attractor and flexible side chain methods. *Protein Science*, 25(1): 295-301.
- 43. Hevener, K. E., Zhao, W., Ball, D. M., Babaoglu, K., Qi, J., White, S. W., and Lee, R. E. (2009). Validation of Molecular Docking Programs for Virtual Screening against Dihydropteroate Synthase. *Journal of Chemical Information and Modeling*, 49(2): 44-460.
- 44. Khalili, N. S. D., Khawory, M. H., Salin, N. H., Zakaria, I. I., Hariono, M., Mikhaylov, A. A., Kamarulzaman, E. E., A Wahab, H., Supratman, U.,

- and Nurul Azmi, M. (2024). Synthesis and biological activity of imidazole phenazine derivatives as potential inhibitors for NS2b-NS3 dengue protease. *Heliyon*, 10(2): e24202.
- 45. Terefe, E. M., and Ghosh, A. (2022). Molecular docking, validation dynamics simulations, and pharmacokinetic prediction of pharmacokinetic prediction of phytochemicals isolated from *Croton dichogamus* against the HIV-1 reverse transcriptase. *Bioinformatics and Biology Insight*, 16: 1179322221125605.
- Ivona, L. and Karelson, M. (2022). The impact of software used and the type of target protein on molecular docking accuracy. *Molecule*, 27(4): 9041.
- 47. Thioguanine Hariono, M., Choi, S. B., Roslim, R. F., Nawi, M. S., Tan, M. L., Kamarulzaman, E. E., Mohamed, N., Yusof, R., Othman, S., Abd Rahman, N., Othman, R., and Wahab, H. A. (2019). Thioguanine-based DENV-2 NS2B/NS3 protease inhibitors: Virtual screening, synthesis, biological evaluation and molecular modelling. *PloS one*, 14(1): e0210869.
- 48. Purohit, P., Sahoo, S., Panda, M., Sahoo, P. S., and Meher, B. R. (2022). Targeting the DENV NS2B-NS3 protease with active antiviral phytocompounds: Structure-based virtual screening, molecular docking and molecular dynamic simulation studies. *Journal of Molecular Modeling*, 28(11): 365.
- 49. Anupurath, S., Rajaraman, V., Gunasekaran, S., Krishnan, A., Sreedevi, S. M., Vinod, S. M.,

- Dakshinamoorthi, B. M., and Rajendran, K. (2021). Electrochemical investigation and molecular docking technique on the interaction of acridinedione dyes with water-soluble nonfluorophic simple amino acids. *ACS Omega*, 6: 30932-30941.
- 50. Lipinski, C. A. (2004). Lead- and drug-like compounds: the rule-of-five revolution. *Drug Discovery: Today Technologies*, 1(4): 337-341.
- 51. Vishvakarma, V.K., Patel, R., Kumari, K., and Sin gh P. (2017). Interaction between bovine serum alb umin and gemini surfactants using molecular docking characterization, *Information Sciences Letters*, 3 (2017): 1-9.
- Veber, D. F., Johnson, S. R., Cheng, H. Y., Smith, B. R., Ward, K. W., and Kopple, K. D. (2002). Molecular properties that influence the oral bioavailability of drug candidates. *Journal of Medicinal Chemistry*, 45(12): 2615-2623.
- 53. Kenny P. W. (2022). Hydrogen-bond donors in drug design. *Journal of Medicinal Chemistry*, 65(21): 14261-14275.
- 54. Khan, S. A., Kumar, S., and Maqsood, A. M., (201 3). Virtual screening of molecular properties and bi oactivity score of boswellic acid derivatives in sear ch of potent anti-inflammatory lead molecule, *International Journal of Interdisciplinary and Multidisc iplinary Studies*, 1: 8-12.
- 55. Halder, A. K., Moura and Cardeiro, M. N. D. S. (2018). QSAR modelling: A therapeutic patent review 2010-present. *Expert Opinion on Therapeutic Patents*, 28(6): 467-476.